

## Direct Photon Production at Next-to-Next-to-Leading Order

John M. Campbell,<sup>1,\*</sup> R. Keith Ellis,<sup>2,†</sup> and Ciaran Williams<sup>3,‡</sup>

<sup>1</sup>*Fermilab, P.O. Box 500, Batavia, Illinois 60510, USA*

<sup>2</sup>*Institute for Particle Physics Phenomenology, Department of Physics, University of Durham, Durham, DH1 3LE, United Kingdom*

<sup>3</sup>*Department of Physics, University at Buffalo, The State University of New York, Buffalo, New York 14260, USA*

(Received 10 January 2017; revised manuscript received 23 February 2017; published 31 May 2017)

We present the first calculation of direct photon production at next-to-next-to-leading order (NNLO) accuracy in QCD. For this process, although the final-state cuts mandate only the presence of a single electroweak boson, the underlying kinematics resembles that of a generic vector boson plus jet topology. In order to regulate the infrared singularities present at this order, we use the  $N$ -jettiness slicing procedure, applied for the first time to a final state that at the Born level includes colored partons but no required jet. We compare our predictions to ATLAS 8 TeV data and find that the inclusion of the NNLO terms in the perturbative expansion, supplemented by electroweak corrections, provides an excellent description of the data with greatly reduced theoretical uncertainties.

DOI: 10.1103/PhysRevLett.118.222001

**Introduction.**—Direct (or inclusive) photon production at hadron colliders provides an excellent testing ground for probing the predictions of the standard model (SM) in fine detail. The LHC, which is currently in its second major data-taking period, provides a powerful tool to study this process [1–4]. For the first time, the experimental uncertainties are under such good control that, over a large region of phase space, they are significantly smaller than the corresponding theoretical ones. Additionally, the most recent data from the LHC highlight the fact that existing theoretical tools are inadequate for describing the experimental measurements [4].

This remarkable achievement of experimental science challenges the theoretical community to provide more sophisticated predictions that have theoretical errors commensurate with the errors in the data. Given the special nature of this final state, the poor description provided by existing theoretical predictions for this channel has serious ramifications for the LHC program. Direct photon production ( $pp \rightarrow \gamma + X$ ) and the associated process in which a jet is explicitly reconstructed ( $pp \rightarrow \gamma + j$ ) are the highest-rate electroweak processes at the LHC. As such, they represent critical standard candles for the exploration of the SM at the LHC. For instance, measurements over a wide range of kinematic configurations—corresponding to different rapidities and transverse momenta of the photon—could be used to provide a precision probe of parton distribution functions (PDFs) [5]. However, up to now, the large theoretical uncertainty has meant that these data are not routinely used in fits. Moreover, the similarity of this process to  $Z + \text{jet}$  production can also be exploited to provide a better understanding of the  $Z(\rightarrow \nu\bar{\nu}) + \text{jet}$  process, which gives rise to leading backgrounds in searches for dark matter and supersymmetry. This is especially useful in the high transverse momentum region,

where there are limited experimental data from the process  $pp \rightarrow Z(\rightarrow \ell^+ \ell^-) + X$  [6].

Over the past 15 years, the theoretical benchmark for direct photon studies has been the next-to-leading-order (NLO) Monte Carlo code JETPHOX [7]. Recent calculations, implemented in the code PETER, have extended the NLO prediction to include both threshold resummation at the next-to-next-to-next-to-leading-logarithmic accuracy ( $N^3\text{LL}$ ) and electroweak Sudakov corrections at leading-logarithmic accuracy [8]. By including the resummed terms, the agreement with the data is somewhat improved, compared to the pure NLO prediction.

It is clearly highly desirable to have a next-to-next-to-leading order (NNLO) prediction for direct photon production that can be compared with LHC data. This is the primary aim of this Letter. Although direct photon production can be defined merely through fiducial cuts on the photon, it proceeds at LO in the perturbation theory through the recoil of the photon against a quark or gluon. Therefore, the underlying structure of the calculation is almost identical to that of the  $\gamma + j$  process. The presence of a final-state colored parton means that a NNLO calculation of this process represents a considerable theoretical challenge.

Over the past few years, significant progress has been made in the field of NNLO calculations, allowing for the calculation of processes involving one [9–15] or two [16,17] massless partons in the final state for the first time. One of the developments that has proven very fruitful for computing NNLO corrections is a novel method for regulating the infrared (IR) singular structure known as  $N$ -jettiness slicing (or subtraction). Originally used in a NNLO calculation of top quark decay [18], the method has since been extended and applied to general LHC processes [12,19]. This method splits the phase space into two

components based on the global event shape,  $N$ -jettiness ( $\tau_N$ ) [20]. Crucially, for an  $N$ -jet final state, the double-unresolved IR poles occur when  $\tau_N = 0$ , so that  $\tau_N > \tau_N^{\text{cut}}$  corresponds to a region in which the calculation has at most single-unresolved limits and therefore resembles a NLO calculation. Furthermore, the cross section in the region  $\tau_N < \tau_N^{\text{cut}}$  can be obtained from a factorization formula derived from the soft-collinear effective theory (SCET) [21–25]. The method can therefore be used as a slicing procedure, with the usual caveat that  $\tau_N^{\text{cut}}$  should be taken as small as possible to minimize power corrections to the below-cut factorization theorem. (For recent work on reducing the dependence on the power corrections, see Refs. [26,27].)

*Calculation.*—In this section, we briefly outline the technical details relating to our calculation. In the  $N$ -jettiness slicing approach, the calculation naturally splits into two components, corresponding to the contributions above and below  $\tau_N = \tau_N^{\text{cut}}$ . Below  $\tau_N^{\text{cut}}$ , the factorization theorem of the SCET describes the cross section as a convolution of a process-dependent hard function  $\mathcal{H}$ , with process-independent beam functions  $\mathcal{B}$  that describe initial-state collinear singularities, jet functions  $\mathcal{J}$  for final-state collinear singularities, and a soft function  $\mathcal{S}$  that describes soft radiation. Expansions accurate to  $O(\alpha_s^2)$  that are relevant for our calculation can be found in Refs. [28,29], [30,31], and [32] for the beam, jet, and soft functions, respectively. The process-independent functions have already been used in the calculation of NNLO corrections to the similar  $W + j$  [12] and  $Z + j$  [14] processes. For our purposes, we use the implementation of these contributions in MCFM as outlined in Ref. [14] and also, for the color-singlet case, in Ref. [33]. We have calculated the process-dependent hard function  $\mathcal{H}$  using the results for the double-virtual  $pp \rightarrow \gamma j$  matrix elements, calculated in Ref. [34]. The helicity amplitudes for the  $gg \rightarrow \gamma g$  one-loop contribution, that also enter the hard function, have been computed using analytic unitarity techniques [35–37]. We have checked that we find agreement between the  $N$ -jettiness slicing method and a more traditional Catani-Seymour dipole [38] calculation at NLO.

In addition to the ingredients required from the SCET factorization theorem, we also require the pieces associated with  $\tau_N > \tau_N^{\text{cut}}$ , which corresponds to the NLO calculation of  $\gamma + 2j$ . This process has been studied at NLO in Ref. [6]. We have recomputed the virtual corrections to this process using unitarity methods and checked our calculation using an in-house implementation of the  $D$ -dimensional numerical algorithm described in Ref. [39]. The amplitudes have also been cross-checked numerically at specific phase space points using `M adgraph5_aMC@NLO`[40].

We now turn our attention to the discussion of  $N$ -jettiness slicing for the case at hand. Direct photon production is representative of an interesting class of processes to compute at NNLO, where no final-state jet

is required but the nonzero recoil of the photon mandates some colored radiation in the final state. (Similar studies for inclusive Higgs and  $Z$  boson production at finite  $p_T$  can be found in Refs. [15,41,42].) The  $N$ -jettiness slicing procedure therefore has to be defined in this context. Clearly, the final-state parton will induce singularities at NNLO that cannot be regulated by a cut on 0-jettiness,  $\tau_0$  (for instance, corresponding to the triple-collinear splitting of a final-state parton). Thus, it is clear that a cut must be made on the 1-jettiness event shape variable, which naturally requires a definition of a jet direction  $n_j$ . Therefore, one has to be careful that the regulating variable  $\tau_1^{\text{cut}}$ , which requires a jet definition, does not interfere with the inclusive nature of the final state, which does not.

In order to achieve this, we start with the usual definition of  $\tau_1^{\text{cut}}$ :

$$\tau_1^{\text{cut}} = \sum_{k=1}^M \min_{i=a,b,1} \left\{ \frac{2q_i \cdot p_k}{Q_i} \right\}. \quad (1)$$

This equation involves the momenta of the parton-level configuration,  $\{p_k\}$ , and the set of momenta that is obtained after application of a jet-clustering algorithm,  $\{q_i\}$ . The scale  $Q_i$  is a measure of the jet or beam hardness, which we take as  $Q_i = 2E_i$ . In order to be well defined, the contribution from the jet direction that enters in Eq. (1) must correspond to a sufficiently hard jet. This is guaranteed by the cut on the photon transverse momentum ( $p_T$ ). In the Born phase space, the transverse momentum of the jet clearly balances that of the photon. In the real-virtual phase space, this constraint is somewhat relaxed, so that the transverse momentum of the leading jet is constrained by  $p_T^1 > p_T^{\gamma}/2$ . In the double-real contribution, the constraint is  $p_T^1 > p_T^{\gamma}/3$ . Thus, as long as we consider sufficiently hard photons,  $\tau_1^{\text{cut}}$  is well defined.

A subtlety to this procedure still arises in practice. Although the jet-clustering procedure is used only to identify the jet direction, with no  $p_T$  cut necessary, there is still a dependence on the cone size  $R$ . An example of this dependence is illustrated in Fig. 1, which makes it clear that, depending on the cone size, radiation may or may not be clustered together to form a jet. In the figure, the smaller cone  $R_1$  results in a different jettiness direction than the larger cone  $R_2$ . Crucially, although these two jettiness directions  $n_j^{R_1}$  and  $n_j^{R_2}$  will differ at large  $\tau_1^{\text{cut}}$ , in the limit in which  $\tau_1^{\text{cut}} \rightarrow 0$ , the difference vanishes. Different choices of  $R$  will therefore result in different power corrections at large  $\tau_1^{\text{cut}}$ , but the cross section should become insensitive to this choice in the double-unresolved limit  $\tau_1^{\text{cut}} \rightarrow 0$ .

*Results.*—In order to properly define the process of direct photon production, it is necessary to apply isolation conditions to the photon. In this Letter, we apply the following smooth-cone isolation [43] criterion:

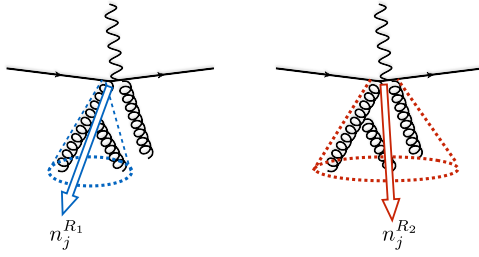


FIG. 1. An illustration of the dependence on  $R$  in the  $N$ -jettiness algorithm. The same event, clustered with two different  $R$  values, results in differing orientations of the jettiness axis. This results in different power corrections for  $\tau_1 > 0$ . In the limit  $\tau_1 \rightarrow 0$ , the dependence on  $R$  vanishes.

$$\sum E_T^{\text{had}}(R) < \epsilon_\gamma E_T^\gamma \left( \frac{1 - \cos R}{1 - \cos R_0} \right)^n \quad \forall R < R_0. \quad (2)$$

This requirement constrains the sum of the hadronic energy inside a cone of radius  $R$ , for all separations  $R$  that are smaller than a chosen cone size  $R_0$ . Note that arbitrarily soft radiation will always pass the condition, but collinear ( $R \rightarrow 0$ ) radiation is forbidden. Therefore, the contributions from collinear fragmentation functions are eliminated. This isolation prescription is therefore highly desirable from a theoretical viewpoint.

Unfortunately, the continuous nature of this isolation prescription cannot be reproduced easily in the experimental setup, in which discrete calorimeter cells are used. Therefore, the smooth-cone procedure is not feasible for use in experimental studies. However, at NLO, it is possible to choose smooth-cone parameters ( $\epsilon_\gamma$ ,  $n$ , and  $R_0$ ) such that the theoretical prediction using smooth-cone isolation is close to the one obtained using fragmentation functions and isolation conditions that mimic the experimental cuts. Such a matching was performed in Ref. [44] for the case of photon pair production. We adopt the same parameters ( $n = 2$ ,  $\epsilon_\gamma = 0.1$ , and  $R_0 = 0.4$ ) that were suggested in that study, finding NLO rates that are within 1%–2% of the JETPHOX [7] results quoted in Ref. [4].

All of the results presented here are for the LHC operating at  $\sqrt{s} = 8$  TeV. The photon is constrained by a simple set of cuts:

$$p_T^\gamma > 65 \text{ GeV}, \quad |\eta_\gamma| < 0.6. \quad (3)$$

The theoretical predictions are all obtained using the CT14 NNLO PDF set [45] with renormalization ( $\mu_R$ ) and factorization ( $\mu_F$ ) scales equal to  $p_T^\gamma$ . When included, PDF uncertainties are quoted at 68% C.L. The rate for this process is proportional to the electromagnetic coupling  $\alpha_{\text{em}}$ . We choose to evaluate  $\alpha_{\text{em}}$  at the scale of the photon transverse momentum, using one-loop running with  $\alpha_{\text{em}}(m_Z) = 1/127.9$ . When we include higher-order electroweak (EW) corrections, they are evaluated at  $\alpha(0) = 1/137$ , appropriate for real photons, so that we

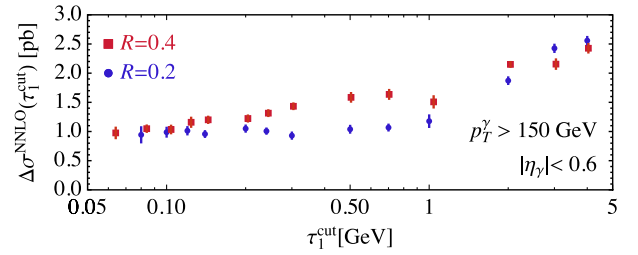


FIG. 2. The dependence of the NNLO coefficient on the parameter  $\tau_1^{\text{cut}}$  and the clustering cone size  $R$ . Two choices are shown corresponding to  $R = 0.4$  (red) and  $R = 0.2$  (blue). The  $R = 0.4$  results have been offset slightly to improve visibility.

are using a modified  $G_\mu$  scheme [46]. As we will shortly observe, this choice is supported phenomenologically by an improved description of the ATLAS data [4,8].

In order to validate our calculation, we first study the dependence of the power corrections on the jet cone size  $R$  that is indicated in Fig. 1. We compute the NNLO coefficient in the perturbative expansion of the cross section ( $\Delta\sigma^{\text{NNLO}}$ ), for anti- $k_T$  jets [47] with  $R = 0.2$  and  $R = 0.4$ , for photons with  $p_T^\gamma > 150$  GeV. Our results are shown in Fig. 2. We observe that for  $\tau_1^{\text{cut}} \gtrsim 0.14$  GeV the power corrections result in predictions for the NNLO coefficient that are quite different for the two values of  $R$ . However, for  $\tau_1^{\text{cut}} \lesssim 0.14$  GeV the predictions tend towards the same result and are in much better agreement. We note that the calculation for  $R = 0.2$  becomes numerically unstable for  $\tau_1^{\text{cut}} < 0.08$  GeV but that the prediction already shows little sensitivity to  $\tau_1^{\text{cut}}$  well before this value is reached.

Given that our calculation is ultimately insensitive to  $R$ , we can thus choose our value to expedite the onset of asymptotic behavior. We thus choose  $R = 0.2$  henceforth. In Fig. 3, we present the  $\tau_1^{\text{cut}}$  dependence for the softer region  $65 < p_T^\gamma < 150$  GeV, which corresponds to the softest photons we study in this Letter. It is clear that the power corrections are sizable for  $\tau_1^{\text{cut}} \gtrsim 0.2$  GeV but that there is little dependence on  $\tau_1^{\text{cut}}$  in the region  $\tau_1^{\text{cut}} \leq 0.1$  GeV. This is in line with the expected scaling from the harder ( $> 150$  GeV) region we studied previously. For our subsequent comparison with the ATLAS data, we set  $\tau_1^{\text{cut}} = \{0.1, 0.2, 0.7\}$  GeV for the phase space regions  $p_T^\gamma > \{65, 150, 470\}$  GeV, respectively.

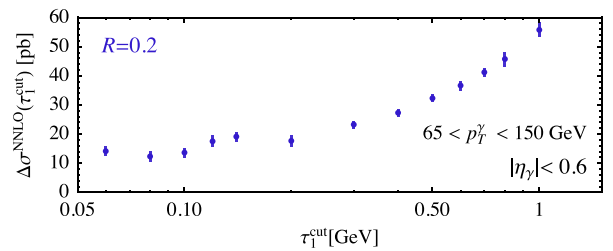


FIG. 3. The dependence of the NNLO coefficient on the parameter  $\tau_1^{\text{cut}}$  for the transverse momentum window  $65 < p_T^\gamma < 150$  GeV.

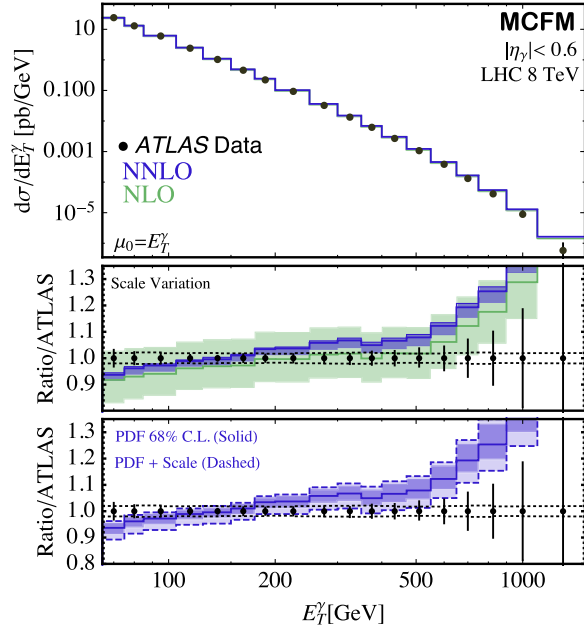


FIG. 4. A comparison of the MCFM predictions for the transverse momentum of the photon to ATLAS 8 TeV data [4]. The middle panel presents the scale variation for NLO and NNLO, while the lower panel shows the combination of PDF and scale uncertainties. The dashed line indicates the experimental luminosity uncertainty.

In Fig. 4, we compare our NNLO (and NLO) predictions from MCFM with 8 TeV ATLAS data [4]. In the middle panel, the shaded bands represent the scale uncertainty, obtained by considering relative deviations using a six-point scale variation about our central choice:  $\{\mu_R, \mu_F\} = \{\lambda_1 p_T^\gamma, \lambda_2 p_T^\gamma\}$  with  $\lambda_i \in \{2, 1, 1/2\}$  and  $\lambda_1 \neq \lambda_2^{-1}$ . It is clear that the scale dependence is greatly reduced for the NNLO prediction when compared to NLO. For the central scale choice, the NNLO prediction is around 5% larger than NLO. The central scale is close to the maximum of the uncertainty band, with deviations around +1% and -4% over much of the range. The tendency of the theoretical prediction to overestimate the data in the high- $p_T$  region is more pronounced when the NNLO correction is included. In the lower panel in Fig. 4, we present the PDF uncertainties and their combination with the scale variation. We observe that the PDF uncertainties are of the same size or larger than the scale variation, particularly at high  $p_T$ . The tension with the data for  $p_T < 100$  GeV is much reduced when the PDF and experimental luminosity errors are included. The fact that the PDF uncertainties are larger than both the scale and experimental uncertainties highlights the potential of this channel to provide invaluable constraints on PDFs in the future. However, there is still significant tension in the  $p_T > 500$  GeV region.

Given the small uncertainty in the NNLO QCD prediction, and the resulting tension with the data, it is especially important to investigate the impact of additional

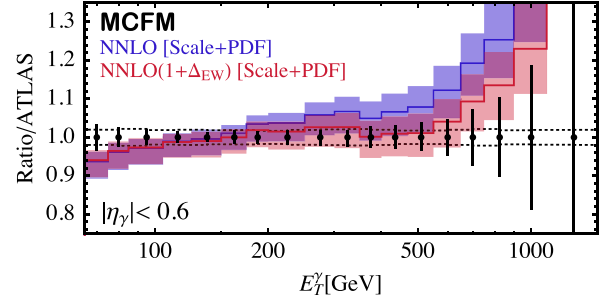


FIG. 5. The effect of including electroweak corrections in addition to the NNLO predictions provided by MCFM, together with scale and PDF (shaded bands) and luminosity (dashed line) uncertainties.

theoretical effects not included in the pure QCD prediction. At high energies it is well known that the impact of Sudakov effects, arising from the virtual radiation of heavy electroweak bosons, is important for this process [8,48–50]. We thus improve our NNLO prediction to include electroweak effects by rescaling it by a factor of  $[1 + \Delta_{EW}]$ , where  $\Delta_{EW}$  is computed using the one-loop high-energy limit expressions of Ref. [48]. (We have checked that an alternate formulation of the EW corrections, that captures the effect of leading-logarithmic electroweak corrections [50], gives practically identical results.)

Accounting for both NNLO QCD and electroweak effects in this way provides the improved prediction shown in Fig. 5. This shows a dramatic improvement in the overall agreement between our theoretical prediction and the data after the inclusion of electroweak effects. The most accurate calculation available until now is one that accounted for threshold resummation to  $N^3LL$  accuracy and electroweak effects [8]. We note in passing that, although the central prediction of that calculation and our NNLO one are similar, the scale uncertainty in the NNLO calculation is around a factor of 3 smaller than the equivalent uncertainty obtained there. We see from Fig. 5 that, after a full accounting of both experimental and theoretical uncertainties has been performed, there is excellent agreement between the NNLO(1 +  $\Delta_{EW}$ ) prediction and the measured distribution for  $E_T^\gamma < 500$  GeV. It is a remarkable feat that the uncertainties are now under good enough control that the inclusion of electroweak corrections becomes mandatory to ensure agreement between the theory and data at energies as low as a few hundred GeV. For  $E_T^\gamma > 500$  GeV the theoretical prediction still appears to overshoot the ATLAS data somewhat, but the two predictions still agree within their respective uncertainties. A preliminary study using a number of alternative PDFs suggests that this disagreement is not a feature of our use of the CT14 PDF set.

*Conclusions.*—We have presented a calculation of direct photon production at NNLO accuracy obtained using the  $N$ -jettiness slicing approach. We compared our prediction

to ATLAS 8 TeV data for  $p_T^{\gamma} > 65$  GeV and  $|\eta_{\gamma}| < 0.6$ . We found that, by combining the NNLO QCD calculation with EW effects, our calculation describes the data very well. Our results represent a significant improvement compared to previous theoretical predictions. The future study of this process, over a wider phase space and at larger center of mass energies, presents an exciting opportunity for precision QCD at colliders. The smallness of the scale variation and experimental uncertainties, set against the sensitivity to PDF uncertainties, underline how useful this channel can be for future PDF fits. In addition, the calculation of ratios of photon momenta for different rapidity regions has interesting potential. The ratios have the advantage of canceling the leading dependence on  $\alpha_{\text{em}}$  and simultaneously the experimental luminosity uncertainty. We leave such detailed phenomenological studies to a future publication.

We are extremely grateful to Radja Boughezal, Xiaohui Liu, and Frank Petriello for providing us with a numerical fit to their calculation of the soft 1-jettiness function that was reported in Ref. [32]. Support provided by the Center for Computational Research at the University at Buffalo. C. W. thanks Sal Rappoccio for providing access to additional CCR computer cores. C. W. is supported by the National Science Foundation through Grant No. PHY-1619877. The research of J. M. C. is supported by the U.S. Department of Energy under Contract No. DE-AC02-07CH11359.

---

\*johnmc@fnal.gov

†keith.ellis@durham.ac.uk

‡ciaranwi@buffalo.edu

- [1] V. Khachatryan *et al.* (CMS Collaboration), *Phys. Rev. Lett.* **106**, 082001 (2011).
- [2] G. Aad *et al.* (ATLAS Collaboration), *Phys. Rev. D* **89**, 052004 (2014).
- [3] S. Chatrchyan *et al.* (CMS Collaboration), *J. High Energy Phys.* **06** (2014) 009.
- [4] G. Aad *et al.* (ATLAS Collaboration), *J. High Energy Phys.* **08** (2016) 005.
- [5] D. d’Enterria and J. Rojo, *Nucl. Phys.* **B860**, 311 (2012).
- [6] Z. Bern, G. Diana, L. J. Dixon, F. Febres Cordero, S. Hoche, H. Ita, D. A. Kosower, D. Maitre, and K. J. Ozeren, *Phys. Rev. D* **84**, 114002 (2011).
- [7] S. Catani, M. Fontannaz, J. Guillet, and E. Pilon, *J. High Energy Phys.* **05** (2002) 028.
- [8] M. D. Schwartz, *J. High Energy Phys.* **09** (2016) 005.
- [9] X. Chen, T. Gehrmann, E. W. N. Glover, and M. Jaquier, *Phys. Lett. B* **740**, 147 (2015).
- [10] A. Gehrmann-De Ridder, T. Gehrmann, E. W. N. Glover, A. Huss, and T. A. Morgan, *Phys. Rev. Lett.* **117**, 022001 (2016).
- [11] R. Boughezal, C. Focke, W. Giele, X. Liu, and F. Petriello, *Phys. Lett. B* **748**, 5 (2015).
- [12] R. Boughezal, C. Focke, X. Liu, and F. Petriello, *Phys. Rev. Lett.* **115**, 062002 (2015).
- [13] R. Boughezal, F. Caola, K. Melnikov, F. Petriello, and M. Schulze, *Phys. Rev. Lett.* **115**, 082003 (2015).
- [14] R. Boughezal, J. M. Campbell, R. K. Ellis, C. Focke, W. T. Giele, X. Liu, and F. Petriello, *Phys. Rev. Lett.* **116**, 152001 (2016).
- [15] A. Gehrmann-De Ridder, T. Gehrmann, E. W. N. Glover, A. Huss, and T. A. Morgan, *J. High Energy Phys.* **07** (2016) 133.
- [16] J. Currie, A. Gehrmann-De Ridder, E. W. N. Glover, and J. Pires, *J. High Energy Phys.* **01** (2014) 110.
- [17] J. Currie, E. W. N. Glover, and J. Pires, *Phys. Rev. Lett.* **118**, 072002 (2017).
- [18] J. Gao, C. S. Li, and H. X. Zhu, *Phys. Rev. Lett.* **110**, 042001 (2013).
- [19] J. Gaunt, M. Stahlhofen, F. J. Tackmann, and J. R. Walsh, *J. High Energy Phys.* **09** (2015) 058.
- [20] I. W. Stewart, F. J. Tackmann, and W. J. Waalewijn, *Phys. Rev. Lett.* **105**, 092002 (2010).
- [21] C. W. Bauer, S. Fleming, and M. E. Luke, *Phys. Rev. D* **63**, 014006 (2000).
- [22] C. W. Bauer, S. Fleming, D. Pirjol, and I. W. Stewart, *Phys. Rev. D* **63**, 114020 (2001).
- [23] C. W. Bauer and I. W. Stewart, *Phys. Lett. B* **516**, 134 (2001).
- [24] C. W. Bauer, D. Pirjol, and I. W. Stewart, *Phys. Rev. D* **65**, 054022 (2002).
- [25] C. W. Bauer, S. Fleming, D. Pirjol, I. Z. Rothstein, and I. W. Stewart, *Phys. Rev. D* **66**, 014017 (2002).
- [26] I. Moul, L. Rothen, I. W. Stewart, F. J. Tackmann, and H. X. Zhu, *Phys. Rev. D* **95**, 074023 (2017).
- [27] R. Boughezal, X. Liu, and F. Petriello, *J. High Energy Phys.* **03** (2017) 160.
- [28] J. R. Gaunt, M. Stahlhofen, and F. J. Tackmann, *J. High Energy Phys.* **04** (2014) 113.
- [29] J. Gaunt, M. Stahlhofen, and F. J. Tackmann, *J. High Energy Phys.* **08** (2014) 020.
- [30] T. Becher and M. Neubert, *Phys. Lett. B* **637**, 251 (2006).
- [31] T. Becher and G. Bell, *Phys. Lett. B* **695**, 252 (2011).
- [32] R. Boughezal, X. Liu, and F. Petriello, *Phys. Rev. D* **91**, 094035 (2015).
- [33] R. Boughezal, J. M. Campbell, R. K. Ellis, C. Focke, W. Giele, X. Liu, F. Petriello, and C. Williams, *Eur. Phys. J. C* **77**, 7 (2017).
- [34] C. Anastasiou, E. W. N. Glover, and M. E. Tejeda-Yeomans, *Nucl. Phys.* **B629**, 255 (2002).
- [35] R. Britto, F. Cachazo, and B. Feng, *Nucl. Phys.* **B725**, 275 (2005).
- [36] P. Mastrolia, *Phys. Lett. B* **678**, 246 (2009).
- [37] S. Badger, *J. High Energy Phys.* **01** (2009) 049.
- [38] S. Catani and M. Seymour, *Nucl. Phys.* **B485**, 291 (1997).
- [39] R. K. Ellis, W. T. Giele, Z. Kunszt, and K. Melnikov, *Nucl. Phys.* **B822**, 270 (2009).
- [40] J. Alwall, R. Frederix, S. Frixione, V. Hirschi, F. Maltoni, O. Mattelaer, H.-S. Shao, T. Stelzer, P. Torrielli, and M. Zaro, *J. High Energy Phys.* **07** (2014) 079.
- [41] X. Chen, J. Cruz-Martinez, T. Gehrmann, E. W. N. Glover, and M. Jaquier, *J. High Energy Phys.* **10** (2016) 066.

- [42] A. Gehrmann-De Ridder, T. Gehrmann, E. W. N. Glover, A. Huss, and T. A. Morgan, *J. High Energy Phys.* **11** (2016) 094.
- [43] S. Frixione, *Phys. Lett. B* **429**, 369 (1998).
- [44] J. M. Campbell, R. K. Ellis, Y. Li, and C. Williams, *J. High Energy Phys.* **07** (2016) 148.
- [45] S. Dulat, T.-J. Hou, J. Gao, M. Guzzi, J. Huston, P. Nadolsky, J. Pumplin, C. Schmidt, D. Stump, and C. P. Yuan, *Phys. Rev. D* **93**, 033006 (2016).
- [46] S. Alioli *et al.*, [arXiv:1606.02330](https://arxiv.org/abs/1606.02330).
- [47] M. Cacciari, G. P. Salam, and G. Soyez, *J. High Energy Phys.* **04** (2008) 063.
- [48] J. H. Kuhn, A. Kulesza, S. Pozzorini, and M. Schulze, *J. High Energy Phys.* **03** (2006) 059.
- [49] T. Becher and X. Garcia i Tormo, *Phys. Rev. D* **88**, 013009 (2013).
- [50] T. Becher and X. Garcia i Tormo, *Phys. Rev. D* **92**, 073011 (2015).